Engineering Conferences International
ECI Digital Archives

5th International Conference on Porous Media and Their Applications in Science, Engineering and Industry

Refereed Proceedings

Summer 6-23-2014

Effective solid-to-fluid heat transfer coefficient in EGS reservoirs

Xiao-Long Ouyang
Tsinghua University

Rui-Na Xu
Tsinghua University

Pei-Xue Jiang
Tsinghua University

Proceedings of the 5th International Conference on Porous Media and its Applications in Science and Engineering
ICPM5
June 22-27, 2014, Kona, Hawaii

EFFECTIVE SOLID-TO-FLUID HEAT TRANSFER COEFFICIENT IN EGS RESERVOIRS

Xiao-Long Ouyang, Rui-Na Xu, Pei-Xue Jiang*
Key Laboratory for Thermal Science and Power Engineering of Ministry of Education
Key Laboratory of CO_2 Utilization and Reduction Technology, Department of Thermal Engineering, Tsinghua University, Beijing, 100084, China

ABSTRACT
The present work developed a three-equation local thermal non-equilibrium model to predict the effective solid-to-fluid heat transfer coefficient in the enhanced geothermal system reservoirs based on the volume averaging method. Due to the high rock-to-fracture size ratio, the solid thermal resistance effect in the internal rocks cannot be neglected in the effective solid-to-fluid heat transfer coefficient. The present three-equation local thermal non-equilibrium model can consider the dynamic variation of the solid thermal resistance in transient heat transfer by introducing the penetration temperature difference. The model was validated by comparison with pore-scale numerical simulations and macro-scale LTNE model numerical simulations. The results show that the three-equation local thermal non-equilibrium model has a high accuracy.

INTRODUCTION
The enhanced geothermal system (EGS) extracts the thermal energy from deep underground dry hot rocks to produce electric power, which is a potential alternative energy in the near future. To achieve this, a coolant fluid will be injected into the reservoirs with dry hot rocks and heated to a higher temperature. This heat transfer process can be simulated by the local thermal non-equilibrium (LTNE) model with considering the solid-to-fluid heat transfer in porous media. In the LTNE model, the solid-to-fluid heat transfer is calculated by the phase volume averaged temperature difference.

However, the classic LTNE model usually neglects the solid thermal resistance in the solid-to-fluid heat transfer coefficient, while the solid thermal resistance plays an important role in the solid-to-fluid heat transfer in EGS. This is because the EGS reservoirs are consist of fractured rocks, where the size of each piece of rock is much larger than that of the fracture. As a result, the rock center temperature can be much higher than the solid-fluid interfacial temperature. The corrected solid-to-fluid heat transfer coefficient with the solid thermal resistance effect is called the effective solid-to-fluid heat transfer coefficient.

There are two main approaches to consider the solid thermal resistance effect in porous media. The first approach is adding a constant correction in the solid-to-fluid heat transfer coefficient:

$$h_{sf}^{-1} = h_{sf,w}^{-1} + \left(\frac{\beta k_s}{d_p} \right)^{-1} \tag{1}$$

where β=6, 8, 10 for slabs, cylinders, and spheres, respectively, by Stuke [1], and β=2(1-ε) by Gelet et al. [2]. This approach is simple but neglects some dynamic information in the transient solid thermal conduction, which will be shown in the following section.

The second approach is coupling the radial heat conduction equation in the particles with the macro-scale energy equation, as by Handley and Heggs [3]. This approach can consider more dynamic information in the transient solid thermal conduction, but requires one more dimension to calculate the radial heat conduction which consumes more calculation time.

With combining these two approaches, the present work will put forward a more precise and efficient model for the effective solid-to-fluid heat transfer coefficient to predict the temperature field in EGS reservoirs based on volume averaging method.

NOMENCLATURE
d_p	=	thickness of the rock slab
h_{sf}	=	Effective solid-to-fluid heat transfer coefficient
$h_{sf,w}$	=	Solid-surface-to-fluid heat transfer coefficient
N	=	fracture number
r	=	Radial coordinate in each piece of rock
T	=	Temperature
$\overline{T}_d$	=	Penetration temperature difference
x	=	x coordinate in macro-scale
y	=	y coordinate in macro-scale
z	=	z coordinate in macro-scale

Greek Symbols

β	=	Coefficient of the solid thermal resistance, defined by Eq. (1)

γ = Constant coefficient of the solid thermal resistance, defined by Eq. (8)

Subscripts

eff	=	Effective
f	=	Fluid phase
s	=	Solid phase
w	=	wall surface of the solid phase

Other

$\overline{\ }$	=	Intrinsic phase average
$\overline{\nabla}$	=	Macro-scale gradient

1 Effective solid-to-fluid heat transfer coefficient model

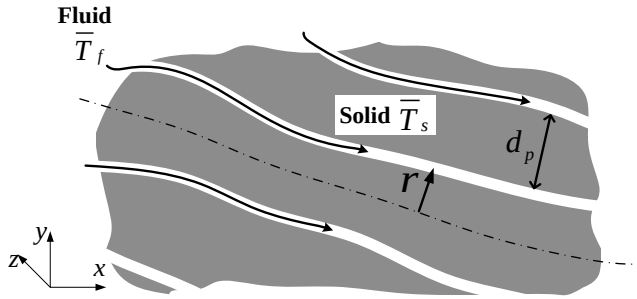

Figure 1: Schematic diagram of uniformly fractured EGS reservoir

The LTNE model in the reservoirs can be expressed as

$$\begin{cases} \varepsilon\rho_f c_{pf}\dfrac{\partial \overline{T}_f}{\partial t}+\rho_f c_{pf}\mathbf{u}\overline{\nabla}\overline{T}_f \\ \qquad\qquad = k_{f,eff}\overline{\nabla}^2\overline{T}_f + ah_{sf}\left(\overline{T}_s-\overline{T}_f\right) \\ \left(1-\varepsilon\right)\rho_s c_{ps}\dfrac{\partial \overline{T}_s}{\partial t} = k_{s,eff}\overline{\nabla}^2\overline{T}_s - ah_{sf}\left(\overline{T}_s-\overline{T}_f\right) \end{cases} \tag{2}$$

where h_{sf} is the effective solid-to-fluid heat transfer coefficient. Here we use the notation, $\overline{\ }$, to distinguish the macro-scale and the pore-scale variables. E.g., $\overline{T}$ is the macro-scale intrinsic phase average of the pore-scale temperature, T. Assume the rocks in porous media are in shape of uniform parallel large slabs with a same thickness of d_p, as shown in Figure 1. In a representative element volume, the local thermal conduction occurs mainly in the radial direction of each piece of rock. Then the transient solid thermal conduction in the internal rocks can be considered based on the second approach mentioned above:

$$\rho_s c_{ps}\frac{\partial T_s}{\partial t} = k_s\frac{\partial^2 T_s}{\partial r^2} \tag{3}$$

Thus, this equation can be related to Eq. (2) with the following boundary conditions:

$$\begin{gathered} -k_s\left.\frac{\partial T_s}{\partial r}\right|_{r=\frac{d_p}{2}} = h_{sf}\left(\overline{T}_s-\overline{T}_f\right)=h_{sf,w}\left(\overline{T}_w-\overline{T}_f\right) \\ T_s\big|_{r=\frac{d_p}{2}}=\overline{T}_w \\ \left.\frac{\partial T_s}{\partial r}\right|_{r=0}=0 \end{gathered} \tag{4}$$

where r is the radial coordinate of each piece of rock, and $\overline{T}_w$ is the averaged wall surface temperature. In addition, $\overline{T}_s$ is the intrinsic phase average of T_s, thus

$$\overline{T}_s = \frac{2}{d_p}\int_0^{\frac{d_p}{2}} T_s dr \tag{5}$$

As a result, the effective solid-to-fluid heat transfer coefficient, h_{sf}, can be derived precisely from Eqs. (2)-(5). However, the pore-scale coordinate, r, brings in one more dimension in the geometry, and Eq. (5) introduces an integral between two variables. These equations are not convenient to solve. To derive more efficient models for h_{sf}, Eqs. (3)-(5) need to be simplified by modeling h_{sf} based on Eq. (1). Note that β in Eq. (1) will be considered as a variable in the following analysis.

1.1 Penetration temperature difference equation

Define the penetration temperature difference:

$$\overline{T}_d = \left(\frac{2}{d_p}\right)^3\int_0^{\frac{d_p}{2}}\left(\overline{T}_s-T_s\right)r^2 dr \tag{6}$$

Here, $\overline{T}_d$ is the volume average of temperature difference, $\overline{T}_s-T_s$, weighted by $(2r/d_p)^2$. Since $(2r/d_p)^2=0$ at the center of the rocks and $(2r/d_p)^2=1$ at the surface of the rocks, $\overline{T}_d$ expresses the divergence between the near-wall temperature and the solid average temperature. It also expresses the penetration degree of surface temperature of the solid phase. Therefore, $\overline{T}_d$ is an important variable to describe the transient solid thermal conduction in macro-scale.

Thus, upscale Eq. (3) with volume averaging and Eqs. (4)-(6) to eliminate the pore-scale coordinate. Then the penetration temperature difference equation can be obtained:

$$\rho_s c_{ps}\frac{\partial \overline{T}_d}{\partial t} = \frac{4}{3}\frac{h_{sf}\left(\overline{T}_s-\overline{T}_f\right)}{d_p}-\frac{8k_s}{d_p^2}\left(\overline{T}_s-\overline{T}_w\right) \tag{7}$$

1.2 Closure modeling and the three-equation LTNE model

To closure the modeling, h_{sf} can be modeled based on Eq. (1). Since β is considered as variable for a more precise model, we propose an assumption that β is reciprocal to the relative penetration temperature difference:

$$\beta = \gamma \left| \frac{\overline{T}_s - \overline{T}_w}{\overline{T}_d} \right| \tag{8}$$

where γ is a constant related to the shape of the rocks. The constant γ can be derived from the exact solution of one-dimensional transient thermal conduction in a large slab. That is

$$\gamma = 4 - \frac{\pi^2}{3} \tag{9}$$

Thus, the three-equation LTNE model is developed based on Eqs. (1), (2), (7) and (8) to consider the transient solid thermal conduction in the internal rocks:

$$\begin{cases} \varepsilon \rho_f c_{pf} \dfrac{\partial \overline{T}_f}{\partial t} + \rho_f c_{pf} \mathbf{u} \overline{\nabla T}_f \\ \qquad = k_{f,eff} \overline{\nabla}^2 \overline{T}_f + a h_{sf} \left(\overline{T}_s - \overline{T}_f \right) \\ (1-\varepsilon) \rho_s c_{ps} \dfrac{\partial \overline{T}_s}{\partial t} = k_{s,eff} \overline{\nabla}^2 \overline{T}_s - a h_{sf} \left(\overline{T}_s - \overline{T}_f \right) \\ \rho_s c_{ps} \dfrac{\partial \overline{T}_d}{\partial t} = \dfrac{4}{3} \dfrac{h_{sf} \left(\overline{T}_s - \overline{T}_f \right)}{d_p} - \dfrac{8 k_s}{d_p^2} \left(\overline{T}_s - \overline{T}_w \right) \end{cases} \tag{10}$$

where the effective solid-to-fluid heat transfer coefficient is modeled as

$$h_{sf}^{-1} = h_{sf,w}^{-1} + \left(\frac{\gamma k_s}{d_p} \left| \frac{\overline{T}_s - \overline{T}_w}{\overline{T}_d} \right| \right)^{-1} \tag{11}$$

the wall surface temperature can be obtained by

$$h_{sf} \left(\overline{T}_s - \overline{T}_f \right) = h_{sf,w} \left(\overline{T}_w - \overline{T}_f \right) \tag{12}$$

Note that the three-equation LTNE model can be used in calculations of one, two or three dimensions in macro-scale. $\overline{T}_s$, $\overline{T}_f$ and $\overline{T}_d$ are the three main variables for the equations.

2 Validation by pore-scale numerical simulations

Figure 2 shows a small enhanced geothermal system with a few artificial fractures in the rocks, whose cross-section area was $W \times W$ and whose length was L. There were N straight fractures opened uniformly parallel to the length direction, whose widths were b. The working fluid, water, flowed through the fractures along the length direction uniformly. The four outer surfaces vertical to the flow direction were covered by insulated walls. The present calculation compares the cases with different fracture number N. For all the cases, these parameters keep the same: W=L=1m, b=1mm, the total flow rate through the system was 0.165kg/s, the initial temperature of the system was 145℃, the inlet fluid temperature was 75℃. The rocks inside the system are assumed impermeable.

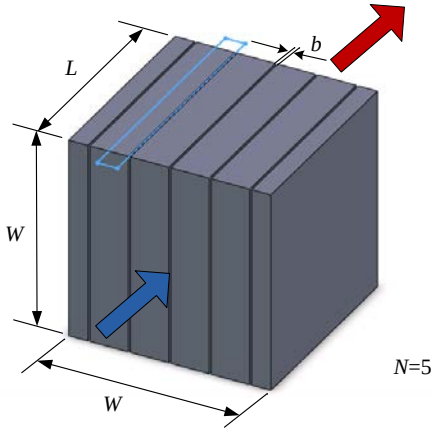

Figure 2: Schematic diagram of the calculation case

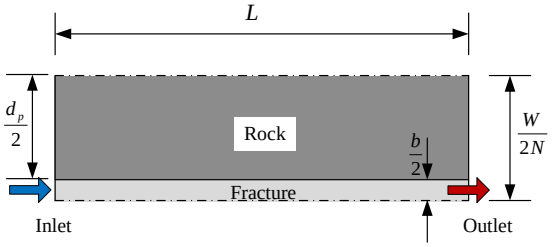

Figure 3: Geometry in the pore-scale numerical simulation

2.1 Pore-scale numerical simulation model

Under these conditions, the pore-scale numerical simulation can be implemented in only a two-dimensional element shown in Figure 2. The geometry of each element is depicted in Figure 3. Half of a rock and half of a fracture with symmetry boundaries were considered in this simulation. Since the fluid velocity in the fracture is slow with the maximum Re=165, the laminar flow momentum equation was occupied to solve the pore-scale flow field, and the transient energy equation to solve the pore-scale temperature field.

2.2 Macro-scale numerical simulation models

For the macro-scale models, one-dimensional flows in the length direction were considered in the governing equations. Because of the narrow fracture, the solid-surface-to-fluid heat transfer coefficient $h_{sf,w}$ is as large as more than 2000W/(m^{2}K), while the solid thermal

resistance is larger than $h_{sf,w}^{-1}$. Thus, $h_{sf,w}^{-1}$ is negligible in this calculation. With this assumption, the one-dimensional three-equation LTNE model can be written as:

$$\begin{cases} \varepsilon\rho_f c_{pf}\dfrac{\partial \overline{T}_f}{\partial t}+\rho_f c_{pf}u\dfrac{\partial \overline{T}_f}{\partial x} \\ \quad =\varepsilon k_f\dfrac{\partial^2 \overline{T}_f}{\partial x^2}+a\dfrac{\gamma k_s}{d_p}\left|\dfrac{\overline{T}_s-\overline{T}_f}{\overline{T}_d}\right|\left(\overline{T}_s-\overline{T}_f\right) \\ (1-\varepsilon)\rho_s c_{ps}\dfrac{\partial \overline{T}_s}{\partial t} \\ \quad =(1-\varepsilon)k_s\dfrac{\partial^2 \overline{T}_s}{\partial x^2}-a\dfrac{\gamma k_s}{d_p}\left|\dfrac{\overline{T}_s-\overline{T}_f}{\overline{T}_d}\right|\left(\overline{T}_s-\overline{T}_f\right) \\ \rho_s c_{ps}\dfrac{\partial \overline{T}_d}{\partial t}=\left(\dfrac{\gamma}{3}\left|\dfrac{\overline{T}_s-\overline{T}_f}{\overline{T}_d}\right|-2\right)\dfrac{4k_s}{d_p^2}\left(\overline{T}_s-\overline{T}_f\right) \end{cases} \tag{13}$$

where the effective thermal conductivity of each phase can be written as the material thermal conductivity multiplied by its volume fraction since the solid and fluid phases are arranged parallel. The thermal dispersion in the effective thermal conductivity of the fluid phase can be neglected due to the fractures are straight.
The initial and boundary conditions:

$$\begin{aligned} &x=0:\quad \overline{T}_f=T_0,\quad \frac{\partial \overline{T}_s}{\partial x}=0 \\ &x=L:\quad \frac{\partial \overline{T}_f}{\partial x}=\frac{\partial \overline{T}_s}{\partial x}=0 \\ &t=0:\quad \overline{T}_f=\overline{T}_s=T_i,\quad \overline{T}_d=0 \end{aligned} \tag{14}$$

where the initial condition $\overline{T}_d=0$ will lead to divergence, in fact $\overline{T}_d$ was set to be a very small value in the numerical calculation. The solid rocks in this system can be regarded as large slabs, thus

$$a=\frac{2N}{W},\quad \varepsilon=\frac{Nb}{W} \tag{15}$$

The local thermal equilibrium (LTE) model and the two-equation LTNE model with Stuke's correlation were also calculated to compare with the three-equation LTNE model. Thus,
The LTE model:

$$\begin{aligned} &\left[\varepsilon\rho_f c_{pf}+(1-\varepsilon)\rho_s c_{ps}\right]\frac{\partial \overline{T}}{\partial t}+\rho_f c_{pf}u\frac{\partial \overline{T}}{\partial x} \\ &\quad =\left[\varepsilon k_f+(1-\varepsilon)k_s\right]\frac{\partial^2 \overline{T}}{\partial x^2} \end{aligned} \tag{16}$$

The two-equation LTNE model with Stuke's correlation:

$$\begin{cases} \varepsilon\rho_f c_{pf}\dfrac{\partial \overline{T}_f}{\partial t}+\rho_f c_{pf}u\dfrac{\partial \overline{T}_f}{\partial x} \\ \quad =\varepsilon k_f\dfrac{\partial^2 \overline{T}_f}{\partial x^2}+a\dfrac{\beta k_s}{d_p}\left(\overline{T}_s-\overline{T}_f\right) \\ (1-\varepsilon)\rho_s c_{ps}\dfrac{\partial \overline{T}_s}{\partial t} \\ \quad =(1-\varepsilon)k_s\dfrac{\partial^2 \overline{T}_s}{\partial x^2}-a\dfrac{\beta k_s}{d_p}\left(\overline{T}_s-\overline{T}_f\right) \end{cases} \tag{17}$$

where β =6 for large slabs. The effective thermal conductivities in Eqs. (16) and (17) are set for the same reasons with the three-equation LTNE model.

2.3 Comparison of results

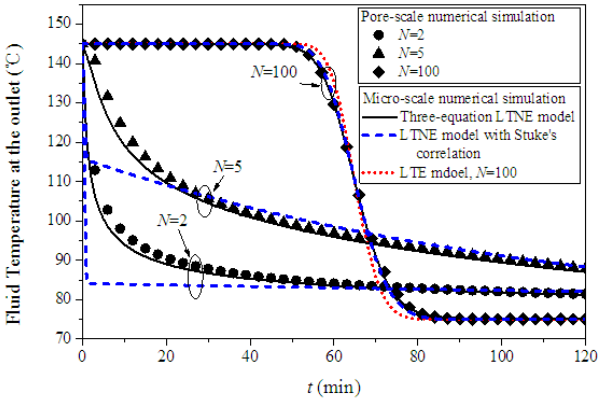

Figure 4: Comparison between the pore-scale and macro-scale numerical simulations

Figure 4 shows the results of the fluid temperature at the outlet. The fracture number density plays an important role on the heat transfer performance of the present system. As shown by the pore-scale numerical simulation result, for the conditions with the constant mass flow rate, the fluid temperature at the outlet keeps the initial temperature for a period and then decreases to the inlet temperature with N=100. However, the fluid temperature at the outlet decreases at the very beginning to a relative low temperature with N=5 or N=2 due to the larger velocity in each fracture. Although the solid-surface-to-fluid heat transfer coefficient $h_{sf,w}$ is large enough, the solid-to-fluid heat transfer ability is still not good enough with a lower fracture number density due to the larger solid thermal resistance in each piece of rock. It is not efficient to extract the thermal energy from the rocks without a large enough fracture number density.
The results of the three-equation LTNE model agree very well with those of the pore-scale numerical simulation. It implies that the three-equation LTNE model has a high accuracy in predicting the transient solid thermal conduction effect in porous media. However, the results of the LTE model can only approach to that of the pore-scale numerical simulation for the case with N=100. It means the case with more fractures such as N=100 approximately satisfies the local thermal equilibrium

condition, while the other two cases do not. It should be noticed that the results of the LTNE model without considering the solid thermal resistance effect in the internal rocks will be the same as those of the LTE model because $h_{sf,w}$ is assumed large enough. Hence, the solid thermal resistance effect in the internal rocks dominates the heat transfer performance with a smaller fracture number density. Therefore, the LTNE model considering the solid thermal resistance effect in the internal rocks must be used for these two cases.

Figure 4 also compares the three-equation LTNE model with the two-equation LTNE model with Stuke's correlation. These two models give largely different predictions of the outlet fluid temperature at the beginning stage with N=5 or N=2. At the later stage, these two predictions are closed while the latter model over-predicts a little. It can be inferred that the constant β in Stuke's correlation cannot predict the dynamic variation of the solid thermal resistance in the beginning stage of transient thermal conduction. But the three-equation LTNE model can overcome this problem by introducing the penetration temperature difference.

CONCLUSIONS

Due to the high rock-to-fracture size ratio in EGS reservoirs, the solid thermal resistance effect in the internal rocks cannot be neglected in the effective solid-to-fluid heat transfer coefficient. The present three-equation local thermal non-equilibrium model can consider the dynamic variation of the solid thermal resistance in transient heat transfer by introducing the penetration temperature difference. The validation shows that the three-equation local thermal non-equilibrium model has a higher accuracy than the two-equation LTNE model with Stuke's correlation, especially at the beginning stage. The results also show that it is not efficient to extract the thermal energy from the rocks without a large enough fracture number density because of the larger solid thermal resistance in the internal rocks.

ACKNOWLEDGEMENT

The authors would like to acknowledge support from the National Natural Science Foundation of China (No. 51276094), the National Science Fund for Creative Research Groups of China (No. 51321002) and the Industrial Technology Development Program (No. B1420110113).

REFERENCES

[1]Stuke B (1948) Berechnung Des Wärmeaustausches in Regeneratoren Mit Zylindrischem Und Kugelförmigem Füllmaterial. Angewandte Chemie 20: 262-268

[2]Gelet R, Loret B, Khalili N (2013) Thermal Recovery From a Fractured Medium in Local Thermal Non-Equilibrium. Int J Numer Anal Met 15: 2471-2501

[3]Handley D, Heggs PJ (1969) The Effect of Thermal Conductivity of the Packing Material On Transient Heat Transfer in a Fixed Bed. Int J Heat Mass Tran 12: 549-570